New Astronomy 55 (2017) 1–12

Contents lists available at ScienceDirect

New Astronomy

journal homepage: www.elsevier.com/locate/newast

Multiple planetary systems: Properties of the current sample

Melissa J. Hobson[a,*], Mercedes Gomez[a,b]

[a] Observatorio Astronómico de Córdoba, Laprida 854, Córdoba, Argentina
[b] CONICET, Consejo Nacional de Investigaciones Científicas y Técnicas, Argentina

HIGHLIGHTS

- Stars hosting multiplanetary systems tend to be less metallic than the Sun.
- More compact systems have more similarly sized planets than low compactness systems.
- Debris disk candidates around stars with multiplanetary systems are identified.

ARTICLE INFO

Article history:
Received 22 August 2016
Revised 13 February 2017
Accepted 14 February 2017
Available online 15 February 2017

Keywords:
(Stars:) planetary systems
Planets and satellites: general
Circumstellar matter
Stars: general

ABSTRACT

We carry out analyses on stellar and planetary properties of multiple exoplanetary systems in the currently available sample. With regards to the stars, we study their temperature, distance from the Sun, and metallicity distributions, finding that the stars that harbour multiple exoplanets tend to have subsolar metallicities, in contrast to metal-rich Hot Jupiter hosts; while non-Hot Jupiter single planet hosts form an intermediate group between these two, with approximately solar metallicities. With regards to the planetary systems, we select those with four or more planets and analyse their configurations in terms of stability (via Hill radii), compactness, and size variations. We find that most planetary pairs are stable, and that the compactness correlates to the size variation: More compact systems have more similarly sized planets and vice versa. We also investigate the spectral energy distributions of the stars hosting multiple exoplanetary systems, seeking infra-red excesses that could indicate the presence of debris disks. These disks would be leftovers from the planetary formation process, and could be considered as analogues of the Solar System's Asteroid or Kuiper belts. We identify potential candidates for disks that are good targets for far infra-red follow-up observations to confirm their existence.

1. Introduction

More than 3400 extrasolar planets and planet candidates are currently known, forming more than 2500 planetary systems. Of these, 575 are multiplanetary systems (as of June 2016, according to *The Extrasolar Planets Encyclopaedia*[1]). In the last two years, the Kepler mission has doubled the sample of known planets and especially of multiplanetary systems, via a technique of statistical validation (Lissauer et al., 2014; Rowe et al., 2014). This increase makes the multiple exoplanetary systems good candidates for initial comparative studies among them.

In this contribution, we present exploratory analyses of stellar and planetary properties of multiple exoplanetary systems in the currently available sample, with the aim of showing their architectures. We caution, however, that this study does not point to a comprehensive and detailed description, since the existence of different biases cannot be disregarded. In spite of this, emerging differences and/or similarities with the Solar System can be identified and kept in mind for future confirmation as the current technical limitations on exoplanet detections are overcome.

Section 2 presents analyses of the properties of the host stars (temperature, distance, and metallicity) and the planetary systems (compactness, stability, and applicability of Titius-Bode 'laws'). In Section 3 we identify debris disks candidates among stars that host multiplanetary systems, via infra-red excesses in their spectral energy distributions. Section 4 presents our conclusions.

2. Analysis

In this work, we divide multiplanetary systems into small systems, defined as those with 2 or 3 planets, and large systems, with 4 or more planets. This division, to some degree, is arbitrary. However, considering that the solar system is the largest planetary system known to date, with eight planets, and as a first try, we define the boundary between what we call small and large sys-

* Corresponding author.
E-mail address: mhobson@oac.unc.edu.ar (M.J. Hobson).

[1] www.exoplanet.eu.

http://dx.doi.org/10.1016/j.newast.2017.02.003

tems at three planets[2]. In total, we have 509 small systems and 66 large systems. We investigate stellar properties, comparing stars that host small and large systems. The aim of this comparison is to investigate whether any differences or similarities emerge between host stars in both groups. We delve into the configurations of the large systems, and carry out an initial characterization of their properties such as the compactness and stability of the planetary configurations. Finally, we search for infrared excesses that may indicate the presence of debris disks.

All stellar and planetary data (save where otherwise indicated) were obtained from *The Extrasolar Planets Encyclopaedia*. The statistical analyses were performed with R codes (R Core Team, 2014).

2.1. Stellar properties

2.1.1. Stellar temperature

Save for exceptional cases such as planetary systems in pulsars (e.g. Wolszczan and Frail 1992; Bailes et al. 2011), the majority of stars with detected planets correspond to spectral types M to F, with a predominance of G-type stars (as can be seen in *The Extrasolar Planets Encyclopaedia* data). This is due to search and observation tendencies: on the one hand, G-type stars (such as the Sun) have historically been the most studied, in attempts to find analogues to our planetary system. On the other hand, as these stars possess many narrow metallic lines in their spectra, they are ideal targets for radial velocity searches. For example, the highly successful HARPS planet search constrains its targets to late-F to late-K stars (Mayor et al., 2011).

Transit missions such as Kepler, which monitor all stars in a sector of the sky, do not in principle have such a marked tendency to favour G stars. However, the dip in stellar brightness caused by a transit is proportionally smaller for high-luminosity stars than for low-luminosity ones. Also, as M to F stars are relatively low in mass, the stellar habitability zone[3] is closer to the star, meaning that the probability of finding potentially habitable transiting planets is higher for low-mass stars. Finally, there are more low-mass than high mass stars in the Galaxy.

While *The Extrasolar Planets Encyclopaedia* reports stellar temperatures, they are generally from different sources. Therefore, in order to have a uniform sample, we used four works: Rowe et al. (2014), who provide stellar parameters for a great number of stars from the Kepler sample; Adibekyan et al. (2012), who derive parameters for 1111 target stars for the HARPS planet search; Santos et al. (2013), who determine parameters for 635 stars with planets; and Maldonado et al. (2012), who give parameters for Sun-type stars with debris disks and planets. Santos et al. (2013) shares some stars with all three of the other works, while Adibekyan et al. (2012) and Maldonado et al. (2012) have stars in common with each other. In all cases, the stellar temperatures of these common objects are in agreement within error values. For stars not included in any of the four catalogues (8% of the sample), the temperatures reported by *The Extrasolar Planets Encyclopaedia* were used. Finally, any stars listed in *The Extrasolar Planets Encyclopaedia* as belonging to an evolved spectral class were removed from consideration.

Fig. 1 shows histograms of stellar temperature for small and large systems. In both cases, the temperatures correspond to stars with spectral types M to F, and G-type stars are predominant. The mean temperatures are 5479 K for stars with small systems, and 5387 K for stars with large systems. The temperature distributions are not statistically different, which probably reflects the bias of radial velocity and transit techniques towards solar spectral types. In the future, improving our capability to detect planets around earlier and later spectral types should probably show a preference of larger planetary systems to be located around earlier and more massive host stars; these have more massive disks, from which more planets can be formed. Current works hint at a positive correlation between stellar mass and primordial disk mass (e.g., Greaves 2010; Andrews et al. 2013; Ansdell et al. 2016), in addition to the known correlation between the mass of the host stars and the occurrence of giant planets (e.g., Johnson et al. 2007; Gaidos et al. 2013). However, it must also be noted that the lifetime of massive disks is shorter, which may limit the formation of massive planets (e.g. Ribas et al. 2015).

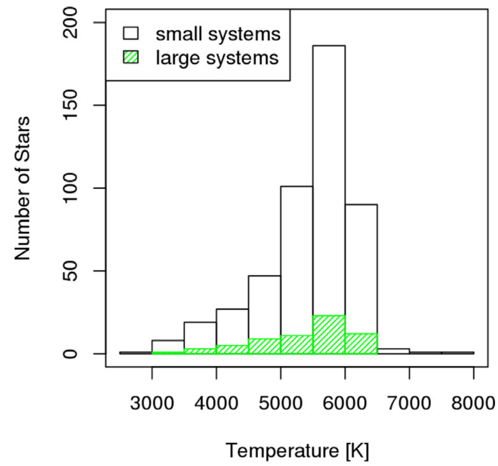

Fig. 1. Histograms of stellar temperature for small systems (2-3 planets) and large systems (4 or more planets).

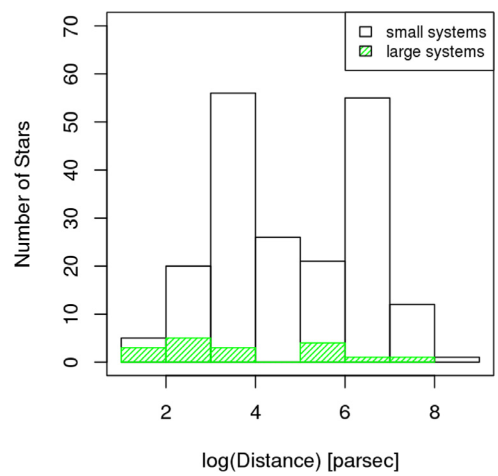

Fig. 2. Stellar distance histograms for small systems (2 to 3 planets) and large systems (4 or more planets).

2.1.2. Stellar distance

Most detection techniques are only effective for relatively close stars. As an example, Kepler reaches magnitude ∼15, which is equivalent (for Sun-like stars) to a distance of some 1100 parsec; but this is an upper limit, and most Kepler systems are much closer, with a median distance of 700 parsec. Most transit-detected planetary candidates are within this range, save those detected by the SWEEPS mission which surveyed a field in the Sagittarius I window of the Galactic Bulge (Sahu et al., 2006); the same applies to radial velocity-detected planets. The timing technique has allowed the detection of planets around more distant stars, some at more than 3000 parsec, the furthest known being the single

---

[2] Among the largest extrasolar planetary systems known, we can mention Kepler 90, with 7 transiting planets (Lissauer et al. 2014; Cabrera et al. 2014), and HD 10180 that may have evidence for as many as 9 planets (Tuomi 2012).

[3] Range of distances from the star such that a planet within them can possess liquid water on its surface.

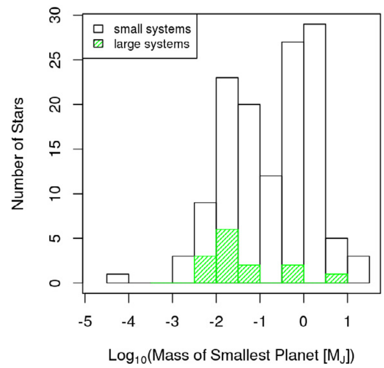

(a) Planetary mass histograms for the smallest planets of small systems (2 to 3 planets) and large systems (4 or more planets) with known masses and stellar distances.

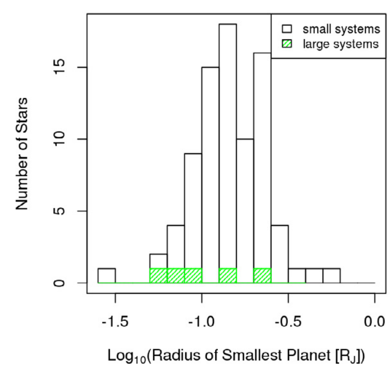

(b) Planetary radius histograms for the smallest planets of small systems (2 to 3 planets) and large systems (4 or more planets) with known radii and stellar distances.

Fig. 3. Planetary size histograms for the smallest planets of small systems (2 to 3 planets) and large systems (4 or more planets) with known stellar distances, separated by masses and radii. It can be seen that in both cases, the distributions for large systems are centred around smaller planetary sizes than those for small systems.

planet PSR B1620-26 b at 3800 parsec (Thorsett et al., 1993). However, the technique with the longest range is that of gravitational microlensing, through which several planets at distances of more than 4000 parsec have been detected, including the most distant multiple system (OGLE-2012-BLG-0026L at 4800 parsec, Han et al. 2013).

Fig. 2 shows log(stellar distance) histograms for small systems – mean distance $\overline{d} = 123$ parsec – and large systems - mean distance $\overline{d} = 45$ parsec. All distances were taken from *The Extrasolar Planets Encyclopaedia*, which provides distances for 196 (39%) of our small systems and 17 (26%) of our large systems. The two peaks clearly visible in the histograms (particularly in those for small systems) correspond to planets detected by the radial velocity and transit techniques respectively.

The distance distributions in Fig. 2 are statistically different ($p - value = 0.01$); however, this is almost certainly due to selection effects. Larger or more massive planets are easier to detect. Consequently, it is reasonable to assume that these planets are found first. In a planetary system with a given number of planets, the probability of detecting an additional (smaller or less massive) one increases with the closeness of the host stars to the Sun. The smaller mean distance of large systems reflects this fact.

Fig. 3 shows histograms of the radius and mass distributions of the smallest or less massive planets in large and small planetary systems with known stellar distances. The medians are: for radii of smallest planets, 0.099 R_J for large systems and 0.144 R_J for small systems; for masses of least massive planets, 0.024 M_J for large systems and 0.265 M_J for small systems. On average, for small planetary systems with known stellar distances, the smallest or less massive planets are larger or more massive than for large planetary systems with known stellar distances, implying they can be detected from a larger distance. This conclusion also holds if we analyse the distributions of all known systems, including those without known stellar distances.

2.1.3. Stellar metallicity

Gonzalez (1997) studied four stars hosting planetary candidates (υ And, τ Boo, 55 Cnc and 51 Peg), finding in all cases that they possessed high metallicities in comparison to nearby stars. This was the first evidence for a planet-metallicity correlation: stars with planets tending to be more metallic than the Sun. Fischer and Valenti's (2005) on a far larger sample showed the same tendency. However, later works (e.g. Udry and Santos 2007) found that this relation is strong only for giant planets close to their host stars, that is for Hot Jupiters.[4]

The situation for Neptune and Earth type planets is not so clear. In their analysis of the 304 exoplanets then known, Hébrard et al. (2010) found that planets with masses below $20M_{\oplus}$ were more numerous around low-metallicity stars. They also reported a tendency of low-mass planets to be preferentially found in multiple systems. While Neves et al. (2013) found a flat relation which hints of an anti-correlation between the presence of these planets and stellar metallicity, Wang and Fischer (2015) found that these planets (as well as gas giants) are more common around metal-rich than metal-poor stars, though the correlation is weaker than for gas giants. Buchhave and Latham (2015), meanwhile, found a metallicity distribution that does not differ from that of stars without planets for the Kepler sample. Zhu et al. (2016) explain the discrepancies between the last two studies by noting various systematic effects in both works, on one hand, and the high occurrence and low detection efficiency of small planets in general, on the other. They conclude that a planet-metallicity correlation for small planets with the same form as that for giant planets cannot be ruled out.

Taking this framework into account, we elected to compare stellar metallicities not only between small and large systems, but also with single-planet systems, discriminating between those with Hot Jupiters and those without. It is important to note here that most multiplanetary systems do not contain Hot Jupiters; likewise, Hot Jupiters are generally alone in their systems (Latham et al., 2011).

Though *The Extrasolar Planets Encyclopaedia* reports stellar metallicities, they are generally from different sources. Therefore, in order to have a uniform sample, we used the same four works cited in Section 2.1.1. There are sufficient common objects between Santos et al. (2013) and Rowe et al. (2014), Santos et al. (2013) and Adibekyan et al. (2012), and Adibekyan et al. (2012) and Maldonado et al. (2012), to allow for comparison. Linear fits of the reported metallicities for common stars correspond to the equations

$$[Fe/H]_{Santos} = (0.80 \pm 0.16)[Fe/H]_{Rowe} + (0.02 \pm 0.03),$$

$$[Fe/H]_{Santos} = (1.01 \pm 0.01)[Fe/H]_{Adibekyan} + (0.004 \pm 0.001),$$

and

[4] Hot Jupiters are defined as planets with mass $\gtrsim 0.5M_J$ and semi-major axis $\lesssim$ 0.1 AU.

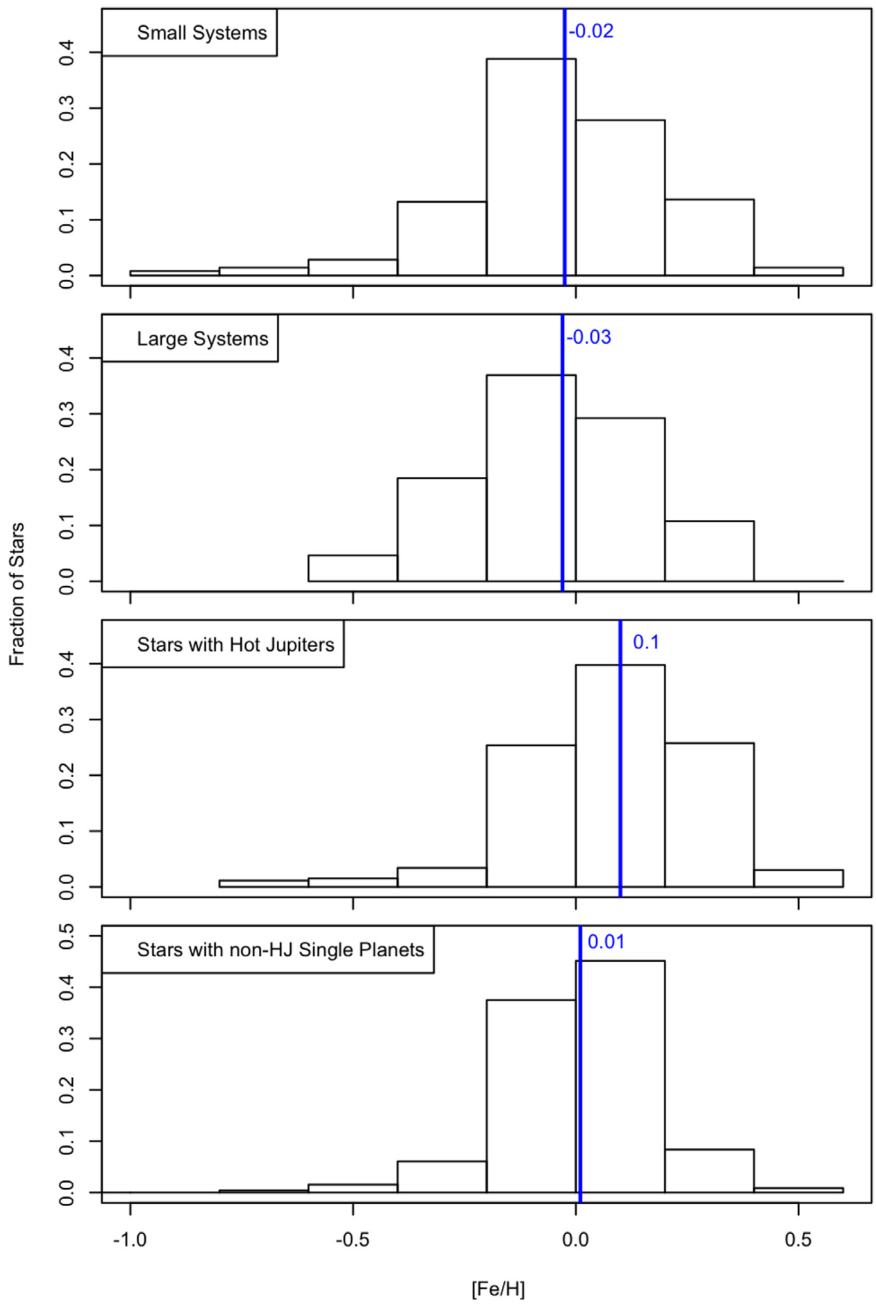

Fig. 4. Metallicity histograms for stars with small systems (top), large systems (second), Hot Jupiters (third), and non-Hot Jupiter single planets (bottom). The vertical blue line indicates the median metallicity for each group.

$[Fe/H]_{Adibekyan} = (0.99 \pm 0.07)[Fe/H]_{Maldonado} + (0.01 \pm 0.02)$ respectively. All are close to the identity equation with a small error range; this suggests that the unification of these catalogues should be fairly homogeneous. Finally, for stars not included in any of the four catalogues, the values reported by *The Extrasolar Planets Encyclopaedia* were used.

Fig. 4 shows metallicity histograms for stars with small systems, large systems, Hot Jupiters, and non-Hot Jupiter single planets. Table 1 gives the mean and median metallicities and standard deviations for each group. For multiple systems both large and small, the average stellar metallicity is sub-solar, whereas for systems with Hot Jupiters it is greater than the Sun's, and for non-Hot Jupiter single planets it is practically solar. The standard deviations, however, are relatively large.

With regards to the cumulative metallicity distributions, the Kolmogorov-Smirnov test (from now, KS test) indicates that the distributions for large and small systems are not significantly different ($p-value = 0.89$). The cumulative distribution for stars with Hot Jupiters, on the other hand, differs significantly from those of both large systems ($p-value = 7.29 \cdot 10^{-5}$) and small systems ($p-value = 8.77 \cdot 10^{-13}$). Likewise, the cumulative distribution for stars with single non-Hot Jupiter planets differs significantly from those of both large systems ($p-value = 0.003$) and small systems ($p-value = 7.62 \cdot 10^{-14}$). Fig. 5 shows the cumulative metallicity distributions for stars with small systems, large systems, Hot Jupiters, and non-Hot Jupiter single planets; around 60% of the stars hosting both small and large systems have sub-zero metallicities, compared to only 40% of those which host Hot Jupiters.

Table 1
Statistics for the four metallicity groups.

Planet(s) hosted	$\overline{[Fe/H]}$	$\widetilde{[Fe/H]}$[a]	$\sigma\,[Fe/H]$	$\widetilde{M}_{largest\ planet}$ $[M_J]$	$\sigma M_{largest\,planet}$ $[M_J]$
Large system	−0.06	−0.03	0.22	0.02	0.54
Small system	−0.03	−0.02	0.25	0.02	1.51
Hot Jupiter	0.09	0.10	0.20	1.17	6.56
Non-Hot Jupiter single	0.01	0.01	0.16	0.02	2.09

[a] $\widetilde{X}$ is the median of X.

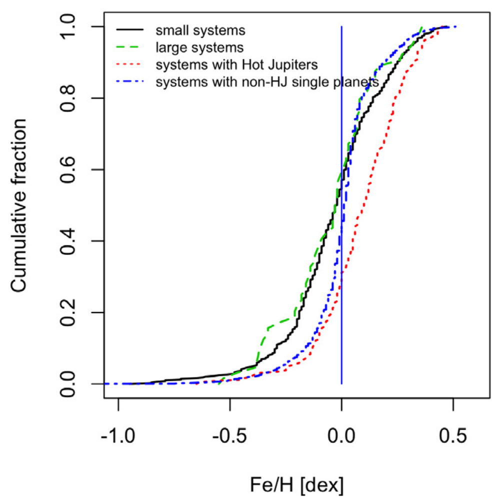

Fig. 5. Cumulative metallicity distributions for stars with large systems (green dashed), small systems (black solid), Hot Jupiters (red dotted), and non-Hot Jupiter single planets (blue dash-dotted). The solid blue vertical line indicates the solar metallicity. 60% of multiplanetary system hosts, 40% of Hot Jupiter hosts and 50% of non-Hot Jupiter single planet hosts, are less metallic than the Sun. (For interpretation of the references to colour in this figure legend, the reader is referred to the web version of this article.)

For single non-Hot Jupiter planet hosting stars, there are equal amounts with sub- and supra-solar metallicities.

To summarize, stars with small and large systems do not differ in metallicity, tending to be less metallic than the Sun. This is in agreement with Hébrard et al.'s (2010) findings that small planets – which are generally found in multiple systems – are more numerous around metal-poor stars. Stars that possess Hot Jupiters, in contrast, are on average more metallic than the Sun, whereas stars with non-Hot Jupiter single planets have on average solar metallicities.

Fig. 6 shows the size distributions of the most massive planet in each system for the small and large systems considered in this work, together with the planetary mass distributions for Hot Jupiters and non-Hot Jupiter single planets. For planets where only the radius is known, we estimated the mass via a simple criterion used by Lissauer et al. (2014):

$$M_p = \left(\frac{R_p}{R_\oplus}\right)^{2.06} M_\oplus \text{ for } R_p > R_\oplus$$

$$M_p = \left(\frac{R_p}{R_\oplus}\right)^{3} M_\oplus \text{ for } R_p < R_\oplus, \quad (1)$$

with $R_\oplus$ and $M_\oplus$ the terrestrial radius and mass respectively.

It can be seen that small planets effectively dominate the distributions for multiple systems (see also Latham et al. 2011). The median values of each distribution are listed in Table 1 and shown in Fig. 6; those for small systems, large systems, and non-Hot Jupiter single planets are identical, although their standard deviations vary. The cumulative planetary mass distributions, however, are significantly different according to the KS test, with that of non-Hot Jupiter single planets covering a wider range of masses than those of the multiple systems (Fig. 7). In particular, the low-mass sections of the distributions differ: the non-Hot Jupiter single planets group has a higher percentage of small planets than the multiple systems. The high-mass sections are not significantly different (according to KS tests performed on subgroups cropped to $M_p > 0.5M_J$). It can also be seen that the distributions for small systems, large systems, and non-Hot Jupiter single planets are much closer to each other than to the distribution for Hot Jupiters.

Thus, it is not surprising that the metallicity distributions of multiple planetary systems (both small and large) are closer to the distribution of single systems without Hot Jupiters than to the distribution of single planetary systems harbouring Hot Jupiters. Additionally, the difference in metallicities between multiple systems and single systems without Hot Jupiters does not appear to be explained simply by a greater presence of giant planets in the second sample.

While some of the 'single-planet' stars considered here may in fact host additional non-detected planets, this should not in principle affect these results: assuming that these 'hidden' multiplanet hosts follow the same trend towards low metallicity found for known multiplanet hosts, their removal from the single-planet hosts samples would if anything shift the mean metallicities of these samples towards higher values. A similar trend can be found in Buchhave and Latham (2015): their original sample of stars with planets included the metallicities of multiplanet-hosting stars repeated by the number of planets each star hosted. When they removed these duplicate values, the average metallicity rose slightly, suggesting that the multiplanetary hosts are effectively less metallic than the single-planet hosts.

In this analysis, therefore, we find that a star does not apparently need to be metal-rich in order to form planetary systems; on the contrary, multiplanetary systems may form around stars of any metallicity, and indeed their hosts tend to be metal-poor. The tendency of Hot Jupiter hosts to be high in metallicity, and the lack of a clear correlation for smaller planets, is explained by accepted planetary formation models such as that of core accretion (e.g. Pollack et al. 1996; Ida and Lin 2004; Mordasini et al. 2012) and tidal downsizing (e.g. Nayakshin and Fletcher 2015).

2.2. Planetary properties

We select the large planetary systems – that is, those with four or more planets – for an initial characterization of their properties.

2.2.1. Hill Radii

If we wish to analyse the structure of the large planetary systems, as will be done in the next two subsections, it is important to first verify that these systems are effectively stable. Therefore, we calculate the separation in Hill radii between adjacent planets.

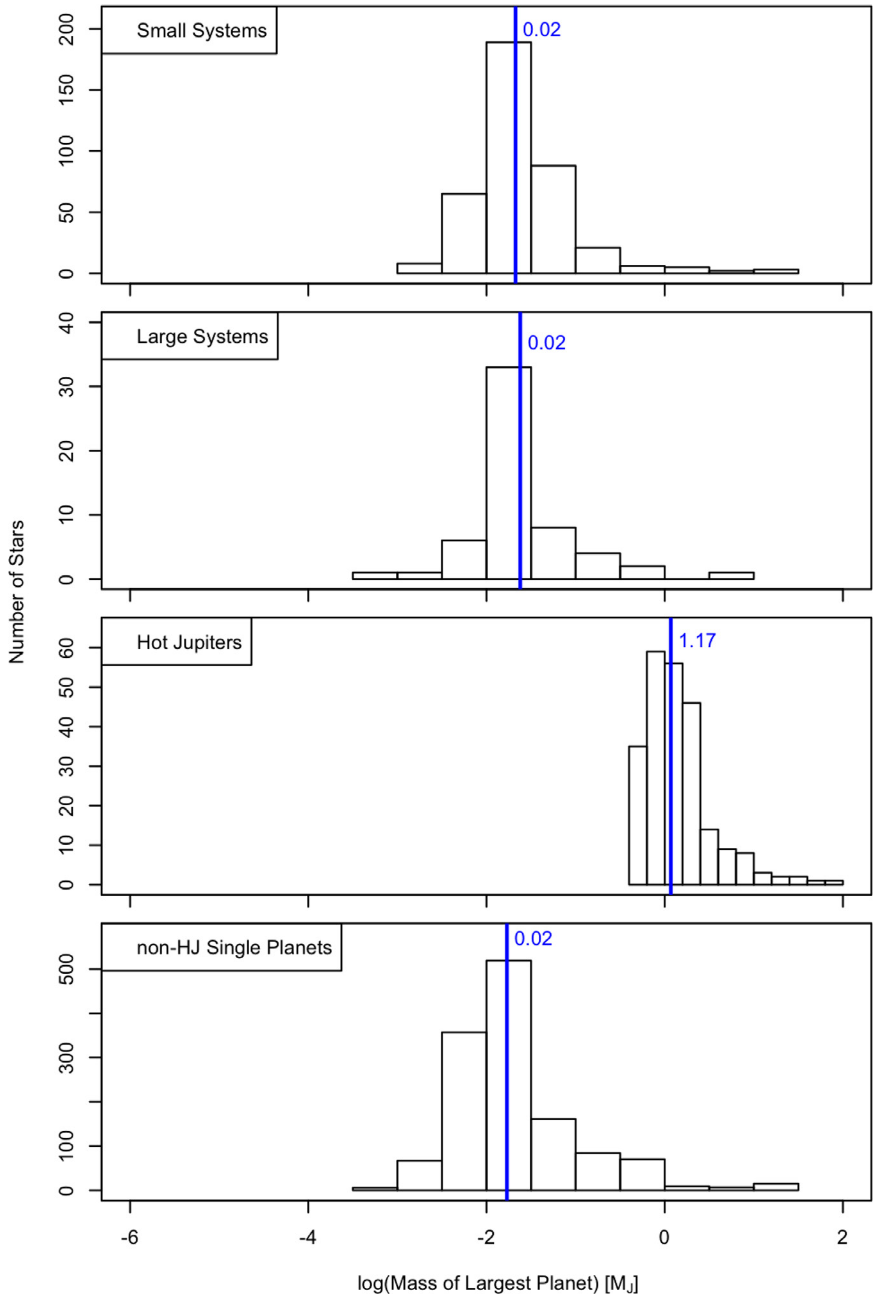

Fig. 6. Size distributions of the most massive planet in each system for stars with large systems (top), small systems (second), Hot Jupiters (third), and non-Hot Jupiter single planets (bottom). The vertical blue line indicates the median mass for each group. (For interpretation of the references to colour in this figure legend, the reader is referred to the web version of this article.)

The Hill radius is defined as

$$R_H = \frac{a_1 + a_2}{2}(\frac{m_1 + m_2}{3M_*})^{\frac{1}{3}}. \quad (2)$$

In order for two adjacent planets to be stable, they must have a minimum separation of, depending on the adopted criteria, 7 R_H (Lovis et al., 2011) to 3.46 R_H (Lissauer et al., 2014).

The separation in Hill radii was calculated for each pair of adjacent planets. As it depends on the planetary mass, it was necessary to estimate it from the planetary radius for those systems where it was not measured. Once again we employed the criterion of Lissauer et al. (2014), given in Section 2.1.3 (Eq. (1)). For 49 of our 66 large systems, all necessary data (stellar mass, planetary mass or radius, semi-major axis) was available directly from the Extrasolar Planets Encyclopaedia. For a further five systems, a search of the literature provided us with the missing data,[5] bringing the total of analysed systems up to 54.

Fig. 8 shows a histogram of the separations in mutual Hill radii for adjacent planetary pairs. Most are effectively stable, though this can only be a tentative result due to the necessity of estimating planetary masses from their radii. Table 2 lists the systems analysed, the stability of the planetary pairs, and notes whether their stability has been previously studied in the literature. Of the 54 systems under consideration, three were not previously analysed:

[5] HD 219134: stellar mass from Motalebi et al. (2015); Kepler-132 : stellar mass from Everett et al. (2015); Kepler-197: stellar mass from Van Eylen and Albrecht (2015); Kepler-296: stellar mass from Torres et al. (2015); Kepler-80: stellar mass and semi-major axes from MacDonald et al. (2016).

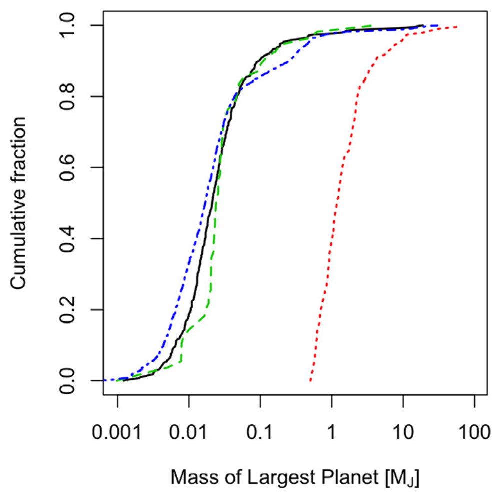

Fig. 7. Cumulative mass distributions of the most massive planet in each system for stars with large systems (green dashed), small systems (black solid), Hot Jupiters (red dotted), and non-Hot Jupiter single planets (blue dash-dotted). (For interpretation of the references to colour in this figure legend, the reader is referred to the web version of this article.)

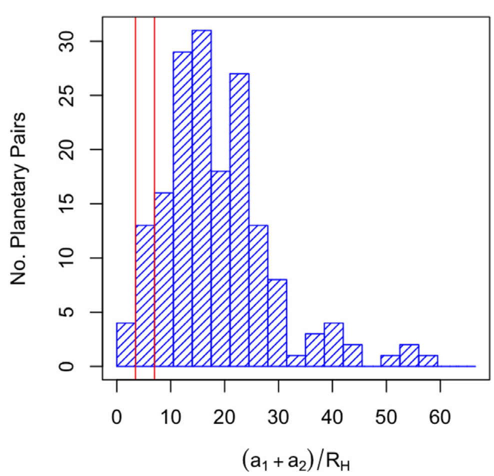

Fig. 8. Histogram of separation in mutual Hill radii for adjacent planetary pairs. The red lines indicate the minimum separation limits of 3.46 and 7 adopted by Lissauer et al. (2014) and Lovis et al. (2011), respectively. The planetary pairs below the 3.46 limit have all been shown to be stable in the literature through detailed orbital analysis. (For interpretation of the references to colour in this figure legend, the reader is referred to the web version of this article.)

GJ 667 C, GJ 676 A, and mu Ara. For GJ 667 C, all adjacent planetary pairs are stable with separations above the $7\,R_H$ limit.

GJ 676 A and mu Ara both have one planetary pair below this limit but above the $3.46\,R_H$ limit. For GJ 676 A, planets b and c are slightly below $7\,R_H$ with a separation of $6.36\,R_H$; however, they are still stable at the $3.46\,R_H$ limit. The other adjacent pairs, d-e and e-b, are well above the $7\,R_H$ limit with separations of $45.27\,R_H$ and $12.42\,R_H$ respectively. Mu Ara b and d are separated by $5.53\,R_H$, while the c-d and b-e pairs have separations of $30.0\,R_H$ and $10.99\,R_H$ respectively.

While the majority of the systems under consideration already had stability analyses in the literature, this uniform study gives us confidence in the reliability of the set of large planetary systems as a whole. It is presented here as a necessary precondition for the subsequent analyses performed on this set.

2.2.2. Compactness

We define 'compactness' as the ratio of the semi-major axis of the innermost planet to that of the outermost planet. Fig. 9

Table 2
Stability of planetary pairs.

Name	Stability[a]	Literature[b]	Name	Stability	Literature
55 Cnc e	a	Lo11	Kepler-256 b	a	R14
55 Cnc	a	Lo11	Kepler-251	a	Li14, R14
GJ 667 C	a		Kepler-256	a	R14
GJ 676 A	b		Kepler-265	a	R14
GJ 876	c	Lo11	Kepler-282	a	Li14, R14
HD 10180	a	Lo11	Kepler-292	a	Li14, R14
HD 141399	b	Vo14	Kepler-296	a	Li14
HD 219134	b	Mo15	Kepler-299	a	R14
HD 40307	a	Lo11	Kepler-304	a	R14
HR 8799	c	Go14, G16	Kepler-306	a	R14
Kepler-102	a	Li14, R14	Kepler-33	b	Li14, R14
Kepler-11	a	R14	Kepler-338	a	R14
Kepler-122	a	Li14, R14	Kepler-341	a	R14
Kepler-132	c	Li14	Kepler-342	a	R14
Kepler-154	a	R14	Kepler-444	a	Ca15
Kepler-167	a	Li14, R14	Kepler-49	a	Li14, R14
Kepler-169	a	R14	Kepler-55	a	Li14, R14
Kepler-172	a	Li14, R14	Kepler-62	a	Li14, R14
Kepler-186	a	Li14, R14	Kepler-79	a	Li14, R14
Kepler-197	a	Li14	Kepler-80	a	Ma16
Kepler-20	b	Li14, R14	Kepler-82	a	Li14, R14
Kepler-208	a	R14	Kepler-84	a	Li14, R14
Kepler-215	a	Li14, R14	Kepler-85	a	R14
Kepler-221	a	R14	Kepler-89	a	Li14, R14
Kepler-224	a	Li14, R14	Kepler-90	b	Li14, R14
Kepler-235	a	Li14, R14	mu Ara	b	
Kepler-238	a	Li14, R14	ups And	b	Lo11
Kepler-245	a	Li14, R14	WASP-47	a	Be15

[a] Stability categories: a: all planetary pairs stable at the $7\,R_H$ separation limit. b: all planetary pairs stable at the $3.46\,R_H$ separation limit. c: at least one planetary pair beneath the $3.46\,R_H$ separation limit.

[b] Li14: Analysed in Lissauer et al. (2014). Lo11: Analysed in Lovis et al. (2011). R14: Analysed in Rowe et al. (2014). Vo14: Analysed in Vogt et al. (2014). Mo15: Analysed in Motalebi et al. (2015). Go14: Analysed in Goździewski and Migaszewski (2014). G16: Analysed in Götberg et al. (2016). Ca15: Analysed in Campante et al. (2015). Ma16: Analysed in MacDonald et al. (2016). Be15: Analysed in Becker et al. (2015).

shows the systems grouped by compactness. More compact systems seem, in this figure, to have more similarly sized planets than less compact ones. Therefore, we define 'size ratio' as the ratio of the size (mass where available, otherwise radius) of the smallest planet to that of the largest planet, and compare the two parameters. As Fig. 10 shows, there is effectively a tendency for more compact systems to have more similarly sized planets and vice versa; a significant linear fit can be found between these parameters ($p - value = 6.25 \times 10^{-7}$). In other words, most compact systems have short period planets (Fig. 9) and also have similar, small sizes (Fig. 10). On the contrary, less compact systems are, in general, composed of larger distant planets and smaller closer planets. These planetary systems tend to have large size-ratios (see Fig. 10). Compact close-packed low mass planetary systems are probably assembled in-situ, since they do not require large amounts of material (e.g. Hansen and Murray 2012; Hansen and Murray 2013; Chiang and Laughlin 2013); whereas larger Jupiter-sized planets, that need more material to be available, are formed further out (e.g. Lin et al. 1996; Ida and Lin 2004).

Our results that more compact systems have more similarly sized planets, and vice versa, contrast with Lissauer et al.'s (2011) finding that neighbouring Kepler planets had large radius ratios when the period ratios were small and vice versa. However, Lissauer et al. (2011) consider all neighbouring pairs of planets in systems with two or more planets, while we are focussing on the closest-furthest and smallest-largest pairs, which are not necessarily neighbouring, for large systems only. In addition, only 10 of the 66 systems with four or more planets we analyse here were known at the time. Ford (2014), on the other hand, notes an abundance of

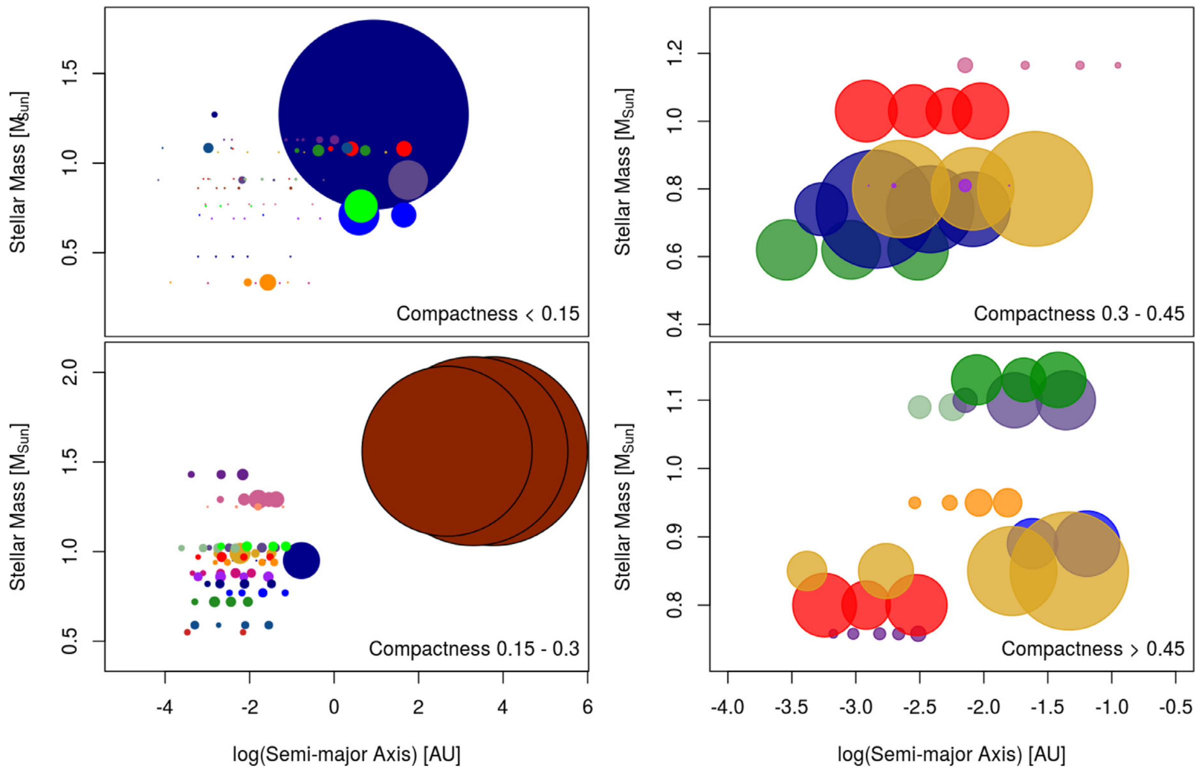

Fig. 9. Planetary systems with four or more planets, grouped by compactness. Each colour represents a planetary system; these are ordered along the vertical axis in each subplot by the mass of the host star. Each circle represents a planet; the location along the horizontal axis corresponds to the logarithm of each planet's semi-major axis, and the circles are proportional to the planetary sizes.

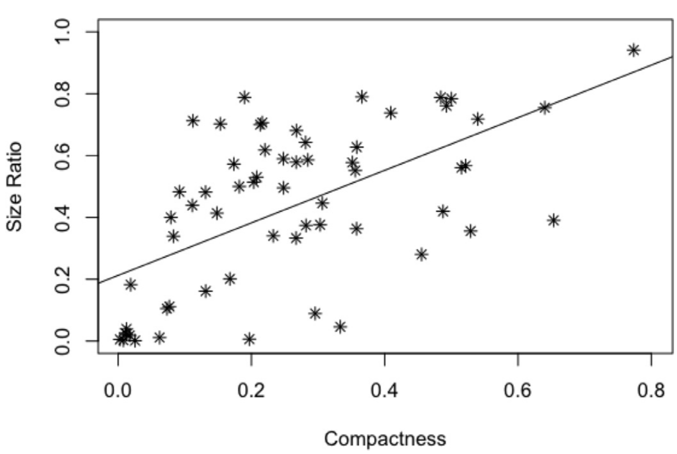

Fig. 10. Size ratio versus compactness for large planetary systems. The line indicates a linear fit.

tightly-packed systems of short-period sub-Neptune planets which show similar planetary sizes. This is in agreement with our positive correlation between high compactness and similarly sized planets.

2.2.3. Titius-Bode 'Laws'

The Titius-Bode 'Law' was proposed for the Solar System as a relation between the semi-major axes of the planetary orbits in the form of a geometric progression:

$$a = c_1 {c_2}^n, \quad (3)$$

where a is the semi-major axis, n is the order number, and c_1 and c_2 are constants. We attempted fits for all our large systems; previously, Lovis et al. (2011) had shown that geometric progressions are good fits to four multiplanetary systems (HD 40307, GJ 581, HD 69830 y HD 10180). To perform the fits, we used the logarithmic form of Eq. (3):

$$log(a) = log(c_1) + n \cdot log(c_2); \quad (4)$$

This allowed us to perform a linear fit on the order number and the logarithm of the semi-major axis. We obtained significant fits ($p-value < 0.1$) for 84% of the systems; all of these have $R^2 > 0.7$, indicating good fits to the data points. In Fig. 11 we show schematic representations of the planets and fits for the systems with the ten lowest p-values.

We emphasize that we do not adjudicate to this 'law' any physical meaning, beyond a simple numerical curiosity; in particular, we must keep in mind the possibility of undetected planets in these systems. Bovaird and Lineweaver (2013) attempted to exploit the Titius-Bode Law as a means of predicting the locations of undetected planets in exoplanetary systems; however, a posterior search by Huang and Bakos (2014) found only five of 97 predicted planets.

3. The search for debris disks

We searched for debris disks around the stars that host multiplanetary systems, by looking for infrared excess in their spectral energy distributions (SEDs). We used the VO Sed Analyzer (VOSA[6]) of the Spanish Virtual Observatory to obtain spectral energy distributions for the 575 multiplanetary systems considered and adjust black-body models. This tool allows the extraction of information from 29 catalogues in wavelengths ranging from the infrared to

[6] Bayo et al. (2008), at http://svo2.cab.inta-csic.es/theory/vosa4/.

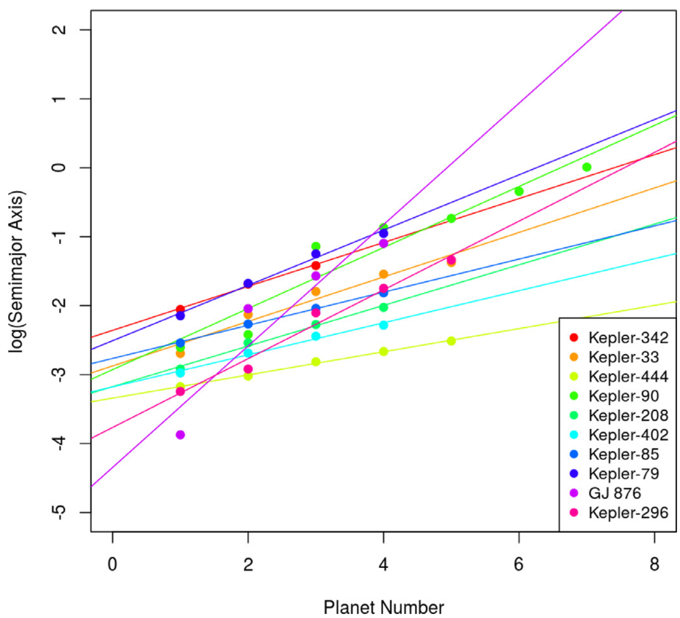

Fig. 11. Schematic representation of the planets (dots) and the Titius-Bode type fits to their positions (lines) for the systems with the ten lowest *p*-values.

the ultraviolet. In the infrared region, it obtains data from WISE[7], IRAS[8], and 2MASS[9], among others.

To apply extinction corrections to the catalogued magnitudes, we used the Everett et al. (2012)[10] determinations for the Kepler planets. For the rest, we derived intrinsic $(B-V)_I$ colours according to their spectral types, adopting the calibration of Kenyon and Hartmann (1995), and calculated the extinction using an average interstellar extinction law: $\frac{A_V}{E(B-V)} = 3.1$, with A_V the extinction and $E(B-V) = (B-V)_O - (B-V)_I$ (Savage and Mathis, 1979).

Once obtained, each SED was examined for IR excess. Excess emission corresponding to potential dust disks was defined as an emission of at least 3 times that predicted by the black-body model at one filter, plus at least 1.5 times the expected flux in one or more additional filters. A visual inspection of all the curves was also performed, to verify that the model curve accurately represented the observed fluxes, and the black-body temperature was checked against the stellar temperature reported in *The Extrasolar Planets Encyclopaedia*.

In Figs. 12 and 13 we show, as examples, two of the obtained SEDs; the first corresponds to HD 204313, which does not show IR excess, and the second to Kepler-186, which shows excess in the W3 (12 µm) and W4 (22 µm) WISE bands.

Unfortunately, our excess emissions come from the WISE and IRAS surveys. However, the IRAS pixel size is so large that we cannot guarantee the IR source is effectively the star. The WISE survey, meanwhile, has recently been shown to be highly contaminated by background emission (see Kennedy and Wyatt 2012, Merín et al. 2014). Searches for debris disks in Kepler candidates using the WISE data were carried out by Lawler and Gladman (2012) and Ribas et al. (2012), but a posterior examination of Ribas et al.'s (2012) candidates by Merín et al. (2014) using the PACS instrument of the Herschel Space Observatory was unable to detect disks in the far IR. We cannot therefore guarantee the existence of these disks; more stringent observations would be necessary. Nevertheless, given the importance of the planet-disk correlation, the identification of candidate debris disks remains an important endeavour.

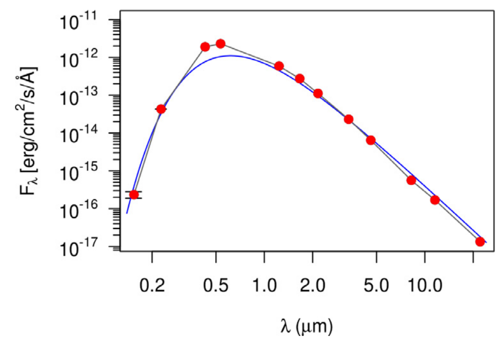

Fig. 12. SED for HD 204313, obtained with VOSA. The red points indicate the observations to which a black-body model (blue curve, corresponding to $T = 4700K$) was fitted. The SED does not show IR excess. (For interpretation of the references to colour in this figure legend, the reader is referred to the web version of this article.)

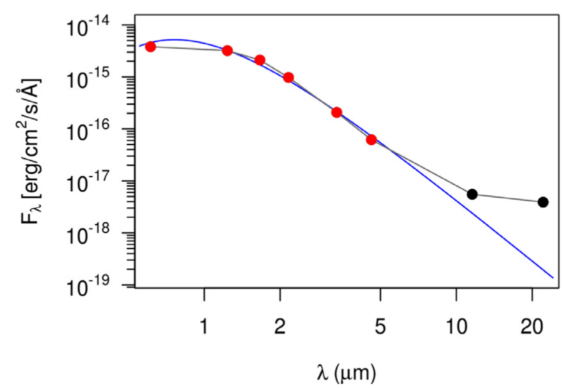

Fig. 13. SED for Kepler-186, obtained with VOSA. The red points indicate the observations to which a black-body model (blue curve, corresponding to $T = 3800K$) was fitted; the black points, IR excess in the W3 (12 µm) and W4 (22 µm) WISE bands. (For interpretation of the references to colour in this figure legend, the reader is referred to the web version of this article.)

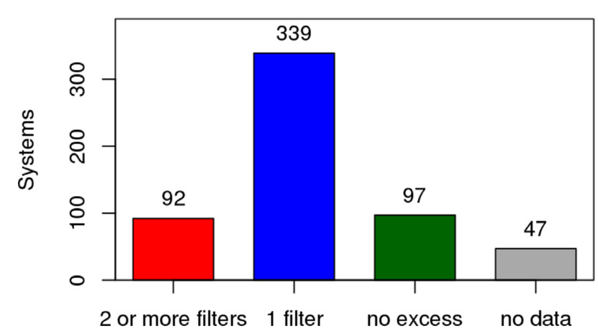

Fig. 14. Multiplanetary systems grouped according to the presence or absence of IR excess in their SEDs.

Fig. 14 shows the number of systems with potential disks (92 systems), with IR excess in a single filter (339 systems, which could also have disks under a less restrictive selection criteria), without excess (97 systems), and without data in VOSA (47 systems). 88 of the 92 systems with potential disks are listed in Table 3; the other four (55 Cnc, Gl 785, HD 99492, and Ups And) have already been discarded as debris disk hosts both by Maldonado et al. (2015) using the IRAS, ISO, and Spitzer telescopes, and by Moro-Martín et al. (2015) using Herschel surveys.

The 88 remaining stars represent an interesting group of candidates for disk hunts using Herschel. Four of them (indicated in Table 3) have recently been confirmed as disk hosts by

[7] Wide-field Infrared Survey Explorer, http://wise.ssl.berkeley.edu/.
[8] Infrared Astronomical Satellite, http://irsa.ipac.caltech.edu/IRASdocs/iras.html.
[9] Two Micron All Sky Survey, http://www.ipac.caltech.edu/2mass/.
[10] Obtained from http://archive.stsci.edu/kepler/kepler_fov/search.php.

Table 3
Stars with potential debris disks.

Star	Maximum excess	Star	Maximum excess	Star	Maximum excess
GJ 682	12 µm (IRAS)	Kepler-224	W4 (WISE)	Kepler-30	W4 (WISE)
GJ 832	60 µm (IRAS)	Kepler-227	W4 (WISE)	Kepler-302	W3 (WISE)
HAT-P-46	60 µm (IRAS)	Kepler-228	W4 (WISE)	Kepler-308	W4 (WISE)
HD 128311[d]	60 µm (IRAS)	Kepler-229	W4 (WISE)	Kepler-315	W4 (WISE)
HD 134606	60 µm (IRAS)	Kepler-234	W4 (WISE)	Kepler-317	W3 (WISE)
HD 141399	100 µm (IRAS)	Kepler-238	W4 (WISE)	Kepler-328	W4 (WISE)
HD 200964	60 µm (IRAS)	Kepler-24	W3 (WISE)	Kepler-344	W4 (WISE)
HD 40307[d,e]	60 µm (IRAS)	Kepler-241	W3 (WISE)	Kepler-349	W3 (WISE)
HD 47366	100 µm (IRAS)	Kepler-245	W3 (WISE)	Kepler-351	W4 (WISE)
HD 52265[d]	100 µm (IRAS)	Kepler-246	W3 (WISE)	Kepler-355	W4 (WISE)
HD 60532	100 µm (IRAS)	Kepler-250	W4 (WISE)	Kepler-357	W4 (WISE)
HD 7924[b]	100 µm (IRAS)	Kepler-254	W4 (WISE)	Kepler-359	W4 (WISE)
HD 96700	60 µm (IRAS)	Kepler-256	W3 (WISE)	Kepler-370	W4 (WISE)
HIP 67851	60 µm (IRAS)	Kepler-257	W4 (WISE)	Kepler-371	W3 (WISE)
HR 228	60 µm (IRAS)	Kepler-259	W4 (WISE)	Kepler-372	W4 (WISE)
HR 8799	100 µm (IRAS)	Kepler-265	W4 (WISE)	Kepler-375	W4 (WISE)
K2-19	W3[a] (WISE)	Kepler-266	W3 (WISE)	Kepler-385	W4 (WISE)
KELT-6	W1[b] (WISE)	Kepler-269	W4 (WISE)	Kepler-392	W3 (WISE)
Kepler-1065	W4[c] (WISE)	Kepler-27	W4 (WISE)	Kepler-395	W3 (WISE)
Kepler-1129	W4 (WISE)	Kepler-273	W4 (WISE)	Kepler-397	W4 (WISE)
Kepler-1245	W4 (WISE)	Kepler-275	W4 (WISE)	Kepler-405	W4 (WISE)
Kepler-1321	W4 (WISE)	Kepler-276	W4 (WISE)	Kepler-436	W3 (WISE)
Kepler-1388	W4 (WISE)	Kepler-281	W4 (WISE)	Kepler-445	W3 (WISE)
Kepler-170	W3 (WISE)	Kepler-284	W4 (WISE)	Kepler-487	W4 (WISE)
Kepler-175	W4 (WISE)	Kepler-286	W4 (WISE)	Kepler-53	W4 (WISE)
Kepler-186	W3 (WISE)	Kepler-291	W4 (WISE)	Kepler-758	W4 (WISE)
Kepler-187	W3 (WISE)	Kepler-292	W4 (WISE)	Kepler-84	W4 (WISE)
Kepler-201	W3 (WISE)	Kepler-294	W4 (WISE)	Kepler-920	W4 (WISE)
Kepler-203	W3 (WISE)	Kepler-299	W4 (WISE)	NY Vir	W4 (WISE)
Kepler-215	W3 (WISE)				

[a] Central wavelength of the W3 filter: 12 µm.
[b] Central wavelength of the W1 filter: 3.4 µm.
[c] Central wavelength of the W4 filter: 22 µm.
[d] Disk detected by Maldonado et al. (2015).
[e] No disk detected by Moro-Martín et al. (2015).

Maldonado et al. (2015), though in one case – HD 40307 – Moro-Martín et al. (2015) do not find a debris disk. However, the vast majority have not yet been examined.

4. Conclusions

In this article, we have described multiplanetary systems and the stars that host them. The stellar temperatures correspond to stars of spectral types M to F. The stars tend to have subsolar metallicities, in contrast to Hot Jupiter hosts, that tend to be metal-rich; while non-Hot Jupiter single planet hosts form an intermediate group between these two, with approximately solar metallicities.

Focussing on systems with four or more planets, we find a relationship between the compactness of the system and the size variations of the planets: more compact systems tend to have less size variation and vice versa. The vast majority of planetary pairs in these systems are stable according to criteria based on the separation in Hill radii, and Titius-Bode type ‘laws’ are generally good fits to the planetary positions.

Finally, we searched for debris disks in these systems via IR excess. We found potential excesses in 92 systems, but recent studies suggest the surveys from which these excesses were drawn may be contaminated by background sources. Therefore, these are only tentative detections; taking into account recent works in the literature, we propose 88 of these systems as candidate disks, four of which have recently been confirmed by Maldonado et al. (2015).

Unfortunately, it is not possible to discard the presence of observational bias in our analysed sample, as all detection techniques have limitations. These results should, therefore, be considered as emerging tendencies that may be confirmed or refuted as improvements in detection techniques allow.

Acknowledgements

We gratefully acknowledge financial support from CONICET (Consejo Nacional de Investigaciones Científicas y Técnicas, Argentina) through grant PIP CONICET No. 11220120100497. This publication makes use of VOSA, developed under the Spanish Virtual Observatory project supported from the Spanish MICINN through grant AyA2011-24052. We thank the anonymous reviewer, whose constructive comments helped to improve the manuscript.

References

Adibekyan, V.Z., Sousa, S.G., Santos, N.C., Delgado Mena, E., González Hernández, J.I., Israelian, G., Mayor, M., Khachatryan, G., 2012. Chemical abundances of 1111 FGK stars from the HARPS GTO planet search program. Galactic stellar populations and planets. A&A 545, A32. doi:10.1051/0004-6361/201219401, arXiv:1207.2388.

Andrews, S.M., Rosenfeld, K.A., Kraus, A.L., Wilner, D.J., 2013. The mass dependence between protoplanetary disks and their stellar hosts. ApJ 771, 129. doi:10.1088/0004-637X/771/2/129, arXiv:1305.5262.

Ansdell, M., Williams, J.P., van der Marel, N., Carpenter, J.M., Guidi, G., Hogerheijde, M., Mathews, G.S., Manara, C.F., Miotello, A., Natta, A., Oliveira, I., Tazzari, M., Testi, L., van Dishoeck, E.F., van Terwisga, S.E., 2016. ALMA survey of lupus protoplanetary disks. I. Dust and gas masses. ApJ 828, 46. doi:10.3847/0004-637X/828/1/46, arXiv:1604.05719.

Bailes, M., Bates, S.D., Bhalerao, V., Bhat, N.D.R., Burgay, M., Burke-Spolaor, S., D'Amico, N., Johnston, S., Keith, M.J., Kramer, M., Kulkarni, S.R., Levin, L., Lyne, A.G., Milia, S., Possenti, A., Spitler, L., Stappers, B., van Straten, W., 2011. Transformation of a star into a planet in a millisecond pulsar binary. Science 333, 1717. doi:10.1126/science.1208890, arXiv:1108.5201.

Bayo, A., Rodrigo, C., Barrado Y Navascués, D., Solano, E., Gutiérrez, R., Morales-Calderón, M., Allard, F., 2008. VOSA: virtual observatory SED analyzer. An application to the Collinder 69 open cluster. A&A 492, 277–287. doi:10.1051/0004-6361:200810395, arXiv:0808.0270.

Becker, J.C., Vanderburg, A., Adams, F.C., Rappaport, S.A., Schwengeler, H.M., 2015. WASP-47: a hot Jupiter system with two additional planets discovered by K2. ApJ 812, L18. doi:10.1088/2041-8205/812/2/L18, arXiv:1508.02411.

Bovaird, T., Lineweaver, C.H., 2013. Exoplanet predictions based on the generalized Titius-Bode relation. MNRAS 435, 1126–1138. doi:10.1093/mnras/stt1357, arXiv:1304.3341.

Buchhave, L.A., Latham, D.W., 2015. The metallicities of stars with and without transiting planets. ApJ 808, 187. doi:10.1088/0004-637X/808/2/187, arXiv:1507.03557.
Cabrera, J., Csizmadia, S., Lehmann, H., Dvorak, R., Gandolfi, D., Rauer, H., Erikson, A., Dreyer, C., Eigmüller, P., Hatzes, A., 2014. The planetary system to KIC 11442793: a compact analogue to the solar system. ApJ 781, 18. doi:10.1088/0004-637X/781/1/18, arXiv:1310.6248.
Campante, T.L., Barclay, T., Swift, J.J., Huber, D., Adibekyan, V.Z., Cochran, W., Burke, C.J., Isaacson, H., Quintana, E.V., Davies, G.R., Silva Aguirre, V., Ragozzine, D., Riddle, R., Baranec, C., Basu, S., Chaplin, W.J., Christensen-Dalsgaard, J., Metcalfe, T.S., Bedding, T.R., Handberg, R., Stello, D., Brewer, J.M., Hekker, S., Karoff, C., Kolbl, R., Law, N.M., Lundkvist, M., Miglio, A., Rowe, J.F., Santos, N.C., Van Laerhoven, C., Arentoft, T., Elsworth, Y.P., Fischer, D.A., Kawaler, S.D., Kjeldsen, H., Lund, M.N., Marcy, G.W., Sousa, S.G., Sozzetti, A., White, T.R., 2015. An ancient extrasolar system with five sub-earth-size planets. ApJ 799, 170. doi:10.1088/0004-637X/799/2/170, arXiv:1501.06227.
Chiang, E., Laughlin, G., 2013. The minimum-mass extrasolar nebula: in situ formation of close-in super-Earths. MNRAS 431, 3444–3455. doi:10.1093/mnras/stt424, arXiv:1211.1673.
Everett, M.E., Barclay, T., Ciardi, D.R., Horch, E.P., Howell, S.B., Crepp, J.R., Silva, D.R., 2015. High-resolution multi-band imaging for validation and characterization of small Kepler planets. AJ 149, 55. doi:10.1088/0004-6256/149/2/55, arXiv:1411.3621.
Everett, M.E., Howell, S.B., Kinemuchi, K., 2012. A UBV photometric survey of the Kepler field. PASP 124, 316–322. doi:10.1086/665529, arXiv:1202.5565.
Fischer, D.A., Valenti, J., 2005. The planet-metallicity correlation. ApJ 622, 1102–1117. doi:10.1086/428383.
Ford, E.B., 2014. Architectures of planetary systems and implications for their formation. Proc. Natl. Acad. Sci. 111, 12616–12621. doi:10.1073/pnas.1304219111, arXiv:1404.3157.
Gaidos, E., Fischer, D.A., Mann, A.W., Howard, A.W., 2013. An understanding of the shoulder of giants: Jovian planets around late K dwarf stars and the trend with stellar mass. ApJ 771, 18. doi:10.1088/0004-637X/771/1/18, arXiv:1305.3228.
Gonzalez, G., 1997. The stellar metallicity-giant planet connection. MNRAS 285, 403–412.
Götberg, Y., Davies, M.B., Mustill, A.J., Johansen, A., Church, R.P., 2016. Long-term stability of the HR 8799 planetary system without resonant lock. A&A 592, A147. doi:10.1051/0004-6361/201526309.
Goździewski, K., Migaszewski, C., 2014. Multiple mean motion resonances in the HR 8799 planetary system. MNRAS 440, 3140–3171. doi:10.1093/mnras/stu455, arXiv:1308.6462.
Greaves, J.S., 2010. Predicting the incidence of planet and debris discs as a function of stellar mass. MNRAS 409, L44–L48. doi:10.1111/j.1745-3933.2010.00943.x, arXiv:1009.2383.
Han, C., Udalski, A., Choi, J.-Y., Yee, J.C., Gould, A., Christie, G., Tan, T.-G., Szymański, M.K., Kubiak, M., Soszyński, I., Pietrzyński, G., Poleski, R., Ulaczyk, K., Pietrukowicz, P., Kozłowski, S., Skowron, J., Wyrzykowski, Ł., OGLE Collaboration, Almeida, L.A., Batista, V., Depoy, D.L., Dong, S., Drummond, J., Gaudi, B.S., Hwang, K.-H., Jablonski, F., Jung, Y.-K., Lee, C.-U., Koo, J.-R., McCormick, J., Monard, L.A.G., Natusch, T., Ngan, H., Park, H., Pogge, R.W., Porritt, I., Shin, I.-G., μ FUN Collaboration, 2013. The second multiple-planet system discovered by microlensing: OGLE-2012-BLG-0026Lb, c – a pair of Jovian planets beyond the snow line. ApJ 762, L28. doi:10.1088/2041-8205/762/2/L28, arXiv:1210.4265.
Hansen, B.M.S., Murray, N., 2012. Migration then assembly: formation of Neptune-mass planets inside 1 AU. ApJ 751, 158. doi:10.1088/0004-637X/751/2/158, arXiv:1105.2050.
Hansen, B.M.S., Murray, N., 2013. Testing in situ assembly with the Kepler planet candidate sample. ApJ 775, 53. doi:10.1088/0004-637X/775/1/53, arXiv:1301.7431.
Hébrard, G., Udry, S., Lo Curto, G., Robichon, N., Naef, D., Ehrenreich, D., Benz, W., Bouchy, F., Lecavelier Des Etangs, A., Lovis, C., Mayor, M., Moutou, C., Pepe, F., Queloz, D., Santos, N.C., Ségransan, D., 2010. The HARPS search for southern extra-solar planets. XX. Planets around the active star BD -08°2823. A&A 512, A46. doi:10.1051/0004-6361/200913525, arXiv:0912.3202.
Huang, C.X., Bakos, G.Á., 2014. Testing the Titius-Bode law predictions for Kepler multiplanet systems. MNRAS 442, 674–681. doi:10.1093/mnras/stu906, arXiv:1405.2259.
Ida, S., Lin, D.N.C., 2004. Toward a deterministic model of planetary formation. I. A desert in the mass and semimajor axis distributions of extrasolar planets. ApJ 604, 388–413. doi:10.1086/381724, arXiv:astro-ph/0312144.
Johnson, J.A., Butler, R.P., Marcy, G.W., Fischer, D.A., Vogt, S.S., Wright, J.T., Peek, K.M.G., 2007. A new planet around an M dwarf: revealing a correlation between exoplanets and stellar mass. ApJ 670, 833–840. doi:10.1086/521720, arXiv:0707.2409.
Kennedy, G.M., Wyatt, M.C., 2012. Confusion limited surveys: using WISE to quantify the rarity of warm dust around Kepler stars. MNRAS 426, 91–107. doi:10.1111/j.1365-2966.2012.21621.x, arXiv:1207.0521.
Kenyon, S.J., Hartmann, L., 1995. Pre-main-sequence evolution in the Taurus-Auriga molecular cloud. ApJS 101, 117. doi:10.1086/192235.
Latham, D.W., Rowe, J.F., Quinn, S.N., Batalha, N.M., Borucki, W.J., Brown, T.M., Bryson, S.T., Buchhave, L.A., Caldwell, D.A., Carter, J.A., Christiansen, J.L., Ciardi, D.R., Cochran, W.D., Dunham, E.W., Fabrycky, D.C., Ford, E.B., Gautier III, T.N., Gilliland, R.L., Holman, M.J., Howell, S.B., Ibrahim, K.A., Isaacson, H., Jenkins, J.M., Koch, D.G., Lissauer, J.J., Marcy, G.W., Quintana, E.V., Ragozzine, D., Sasselov, D., Shporer, A., Steffen, J.H., Welsh, W.F., Wohler, B., 2011. A first comparison of Kepler planet candidates in single and multiple systems. ApJ 732, L24. doi:10.1088/2041-8205/732/2/L24, arXiv:1103.3896.
Lawler, S.M., Gladman, B., 2012. Debris disks in kepler exoplanet systems. ApJ 752, 53. doi:10.1088/0004-637X/752/1/53, arXiv:1112.0368.
Lin, D.N.C., Bodenheimer, P., Richardson, D.C., 1996. Orbital migration of the planetary companion of 51 Pegasi to its present location. Nature 380, 606–607. doi:10.1038/380606a0.
Lissauer, J.J., Marcy, G.W., Bryson, S.T., Rowe, J.F., Jontof-Hutter, D., Agol, E., Borucki, W.J., Carter, J.A., Ford, E.B., Gilliland, R.L., Kolbl, R., Star, K.M., Steffen, J.H., Torres, G., 2014. Validation of Kepler's multiple planet candidates. II. Refined statistical framework and descriptions of systems of special interest. ApJ 784, 44. doi:10.1088/0004-637X/784/1/44, arXiv:1402.6352.
Lissauer, J.J., Ragozzine, D., Fabrycky, D.C., Steffen, J.H., Ford, E.B., Jenkins, J.M., Shporer, A., Holman, M.J., Rowe, J.F., Quintana, E.V., Batalha, N.M., Borucki, W.J., Bryson, S.T., Caldwell, D.A., Carter, J.A., Ciardi, D., Dunham, E.W., Fortney, J.J., Gautier III, T.N., Howell, S.B., Koch, D.G., Latham, D.W., Marcy, G.W., Morehead, R.C., Sasselov, D., 2011. Architecture and dynamics of Kepler's candidate multiple transiting planet systems. ApJS 197, 8. doi:10.1088/0067-0049/197/1/8, arXiv:1102.0543.
Lovis, C., Ségransan, D., Mayor, M., Udry, S., Benz, W., Bertaux, J.-L., Bouchy, F., Correia, A.C.M., Laskar, J., Lo Curto, G., Mordasini, C., Pepe, F., Queloz, D., Santos, N.C., 2011. The HARPS search for southern extra-solar planets. XXVIII. Up to seven planets orbiting HD 10180: probing the architecture of low-mass planetary systems. A&A 528, A112. doi:10.1051/0004-6361/201015577, arXiv:1011.4994.
MacDonald, M.G., Ragozzine, D., Fabrycky, D.C., Ford, E.B., Holman, M.J., Isaacson, H.T., Lissauer, J.J., Lopez, E.D., Mazeh, T., Rogers, L., Rowe, J.F., Steffen, J.H., Torres, G., 2016. A dynamical analysis of the Kepler-80 system of five transiting planets. AJ 152, 105. doi:10.3847/0004-6256/152/4/105, arXiv:1607.07540.
Maldonado, J., Eiroa, C., Villaver, E., Montesinos, B., Mora, A., 2012. Metallicity of solar-type stars with debris discs and planets⋆. A&A 541, A40. doi:10.1051/0004-6361/201218800, arXiv:1202.5884.
Maldonado, J., Eiroa, C., Villaver, E., Montesinos, B., Mora, A., 2015. Searching for signatures of planet formation in stars with circumstellar debris discs. A&A 579, A20. doi:10.1051/0004-6361/201525764, arXiv:1502.07100.
Mayor, M., Marmier, M., Lovis, C., Udry, S., Ségransan, D., Pepe, F., Benz, W., Bertaux, J., Bouchy, F., Dumusque, X., Lo Curto, G., Mordasini, C., Queloz, D., Santos, N.C., 2011. The HARPS search for southern extra-solar planets XXXIV. Occurrence, mass distribution and orbital properties of super-Earths and Neptune-mass planets. ArXiv e-prints arXiv:1109.2497.
Merín, B., Ardila, D.R., Ribas, Á., Bouy, H., Bryden, G., Stapelfeldt, K., Padgett, D., 2014. Herschel/PACS photometry of transiting-planet host stars with candidate warm debris disks. A&A 569, A89. doi:10.1051/0004-6361/201322956, arXiv:1409.0572.
Mordasini, C., Alibert, Y., Benz, W., Klahr, H., Henning, T., 2012. Extrasolar planet population synthesis . IV. Correlations with disk metallicity, mass, and lifetime. A&A 541, A97. doi:10.1051/0004-6361/201117350, arXiv:1201.1036.
Moro-Martín, A., Marshall, J.P., Kennedy, G., Sibthorpe, B., Matthews, B.C., Eiroa, C., Wyatt, M.C., Lestrade, J.-F., Maldonado, J., Rodriguez, D., Greaves, J.S., Montesinos, B., Mora, A., Booth, M., Duchêne, G., Wilner, D., Horner, J., 2015. Does the presence of planets affect the frequency and properties of extrasolar Kuiper belts? Results from the herschel debris and dunes surveys. ApJ 801, 143. doi:10.1088/0004-637X/801/2/143, arXiv:1501.03813.
Motalebi, F., Udry, S., Gillon, M., Lovis, C., Ségransan, D., Buchhave, L.A., Demory, B.O., Malavolta, L., Dressing, C.D., Sasselov, D., Rice, K., Charbonneau, D., Collier Cameron, A., Latham, D., Molinari, E., Pepe, F., Affer, L., Bonomo, A.S., Cosentino, R., Dumusque, X., Figueira, P., Fiorenzano, A.F.M., Gettel, S., Harutyunyan, A., Haywood, R.D., Johnson, J., Lopez, E., Lopez-Morales, M., Mayor, M., Micela, G., Mortier, A., Nascimbeni, V., Philips, D., Piotto, G., Pollacco, D., Queloz, D., Sozzetti, A., Vanderburg, A., Watson, C.A., 2015. The HARPS-N rocky planet search. I. HD 219134 b: a transiting rocky planet in a multi-planet system at 6.5 pc from the Sun. A&A 584, A72. doi:10.1051/0004-6361/201526822, arXiv:1507.08532.
Nayakshin, S., Fletcher, M., 2015. Tidal Downsizing model – III. Planets from sub-Earths to brown dwarfs: structure and metallicity preferences. MNRAS 452, 1654–1676. doi:10.1093/mnras/stv1354, arXiv:1504.02365.
Neves, V., Bonfils, X., Santos, N.C., Delfosse, X., Forveille, T., Allard, F., Udry, S., 2013. Metallicity of M dwarfs. III. Planet-metallicity and planet-stellar mass correlations of the HARPS GTO M dwarf sample. A&A 551, A36. doi:10.1051/0004-6361/201220574, arXiv:1212.3372.
Pollack, J.B., Hubickyj, O., Bodenheimer, P., Lissauer, J.J., Podolak, M., Greenzweig, Y., 1996. Formation of the giant planets by concurrent accretion of solids and gas. Icarus 124, 62–85. doi:10.1006/icar.1996.0190.
R Core Team, 2014. R: A Language and Environment for Statistical Computing. R Foundation for Statistical Computing, Vienna, Austria.
Ribas, Á., Bouy, H., Merín, B., 2015. Protoplanetary disk lifetimes vs. stellar mass and possible implications for giant planet populations. A&A 576, A52. doi:10.1051/0004-6361/201424846, arXiv:1502.00631.
Ribas, Á., Merín, B., Ardila, D.R., Bouy, H., 2012. Warm debris disks candidates in transiting planets systems. A&A 541, A38. doi:10.1051/0004-6361/201118306, arXiv:1203.0013.
Rowe, J.F., Bryson, S.T., Marcy, G.W., Lissauer, J.J., Jontof-Hutter, D., Mullally, F., Gilliland, R.L., Issacson, H., Ford, E., Howell, S.B., Borucki, W.J., Haas, M., Huber, D., Steffen, J.H., Thompson, S.E., Quintana, E., 2014. Validation of Kepler's multiple planet candidates. III. Light curve analysis and announcement of hundreds of new multi-planet systems. ApJ 784, 45. doi:10.1088/0004-637X/784/1/45, arXiv:1402.6534.

Sahu, K.C., Casertano, S., Bond, H.E., Valenti, J., Ed Smith, T., Minniti, D., Zoccali, M., Livio, M., Panagia, N., Piskunov, N., Brown, T.M., Brown, T., Renzini, A., Rich, R.M., Clarkson, W., Lubow, S., 2006. Transiting extrasolar planetary candidates in the Galactic Bulge. Nature 443, 534–540. doi:10.1038/nature05158, arXiv:astro-ph/0610098.

Santos, N.C., Sousa, S.G., Mortier, A., Neves, V., Adibekyan, V., Tsantaki, M., Delgado Mena, E., Bonfils, X., Israelian, G., Mayor, M., Udry, S., 2013. SWEET-Cat: a catalogue of parameters for stars with ExoplanETs. I. New atmospheric parameters and masses for 48 stars with planets. A&A 556, A150. doi:10.1051/0004-6361/201321286, arXiv:1307.0354.

Savage, B.D., Mathis, J.S., 1979. Observed properties of interstellar dust. ARA&A 17, 73–111. doi:10.1146/annurev.aa.17.090179.000445.

Thorsett, S.E., Arzoumanian, Z., Taylor, J.H., 1993. PSR B1620-26 – a binary radio pulsar with a planetary companion? ApJ 412, L33–L36. doi:10.1086/186933.

Torres, G., Kipping, D.M., Fressin, F., Caldwell, D.A., Twicken, J.D., Ballard, S., Batalha, N.M., Bryson, S.T., Ciardi, D.R., Henze, C.E., Howell, S.B., Isaacson, H.T., Jenkins, J.M., Muirhead, P.S., Newton, E.R., Petigura, E.A., Barclay, T., Borucki, W.J., Crepp, J.R., Everett, M.E., Horch, E.P., Howard, A.W., Kolbl, R., Marcy, G.W., McCauliff, S., Quintana, E.V., 2015. Validation of 12 small Kepler transiting planets in the habitable zone. ApJ 800, 99. doi:10.1088/0004-637X/800/2/99, arXiv:1501.01101.

Tuomi, M., 2012. Evidence for nine planets in the HD 10180 system. A&A 543, A52. doi:10.1051/0004-6361/201118518, arXiv:1204.1254.

Udry, S., Santos, N.C., 2007. Statistical properties of exoplanets. ARA&A 45, 397–439. doi:10.1146/annurev.astro.45.051806.110529.

Van Eylen, V., Albrecht, S., 2015. Eccentricity from transit photometry: small planets in Kepler multi-planet systems have low eccentricities. ApJ 808, 126. doi:10.1088/0004-637X/808/2/126, arXiv:1505.02814.

Vogt, S.S., Butler, R.P., Rivera, E.J., Kibrick, R., Burt, J., Hanson, R., Meschiari, S., Henry, G.W., Laughlin, G., 2014. A four-planet system orbiting The K0V Star HD 141399. ApJ 787, 97. doi:10.1088/0004-637X/787/2/97, arXiv:1404.7462.

Wang, J., Fischer, D.A., 2015. Revealing a universal planet-metallicity correlation for planets of different sizes around solar-type stars. AJ 149, 14. doi:10.1088/0004-6256/149/1/14.

Wolszczan, A., Frail, D.A., 1992. A planetary system around the millisecond pulsar PSR1257 + 12. Nature 355, 145–147. doi:10.1038/355145a0.

Zhu, W., Wang, J., Huang, C., 2016. Dependence of small planet frequency on stellar metallicity hidden by their prevalence. ApJ 832, 196. doi:10.3847/0004-637X/832/2/196, arXiv:1605.04310.